

High Temperature Response of Selected Microstructures in Fe-Mn-Cr-Cu Corrosion Resistant Alloy Cast Irons

Vinod Kumar

(Submitted 28 January 2003)

High temperature response was determined by thermo-gravimetric method for the microstructures in the (1) as-cast, (2) 950 °C, 10 h, air cooled, and (3) 1050 °C, 10 h, air cooled conditions for four newly designed cast irons designated as B1 (6Mn-5Cr-1.5Cu), B2 (7.5Mn-5Cr-1.5Cu), B3 (6Mn-5Cr-3.0Cu), and B4 (7.5Mn-5Cr-3.0Cu) and intended to resist aqueous corrosion under marine conditions. The current study was undertaken as corrosion resistant compositions may have potential applications as high temperature materials. It was observed that while the as-cast microstructure was useful only up to 600 °C, the above mentioned heat treatments raised the useful temperature limit of application to ~800 °C. The relative performance of the alloys was a function of the austenite volume fraction and its stability, morphology, and stability of the second phase and the proneness of the alloys to carbide transformation. The data thus obtained is of considerable interest for alloy design in the future as it lays down guidelines for developing modified compositions exhibiting excellent high temperature response.

Keywords alloy cast iron, carbides, high temperature, thermo-gravimetric

1. Introduction

A comprehensive review of the literature on the corrosion resistant alloy cast irons currently in use, namely (1) ferritic (high Si), (2) austenitic (Ni-resist), and (3) martensitic (high Cr with or without Mo), revealed that ferritic irons are most useful under oxidizing conditions. Their poor mechanical strength and shock resistance preclude their general engineering applications.^[1,2] Ni-resistant irons, although very useful in a variety of aqueous environments, have a low strength and are unsuitable at operating temperatures >800 °C.^[2,3] The high Cr irons can be used up to higher service temperatures.^[2] Their shock resistance can be improved by lowering C content.^[4]

A critical analysis revealed that there is a general lack of systematic information on the electrochemical, high temperature, and deformation behavior of microstructures encountered in alloy white irons. An alloy development program based on using Mn, Cr, Cu as alloying elements was therefore initiated to assess whether new meaningful compositions helpful in resisting aqueous corrosion could be developed. Details of the strategies adopted for the design of alloys and experimentation carried out are reported elsewhere.^[5] The alloys were investigated in the as-cast and in the heat-treated conditions to arrive at qualitative interrelations between microstructure and properties. Correlation on corrosion behavior with the microstructure^[6-8] and hardness with the transformation behavior^[9] of the experimental alloys has already been reported.

This paper highlights the high temperature response of selected microstructures, generated in the experimental alloys, through heat treatments.

Vinod Kumar, Product Development Division, R & D Centre for Iron and Steel, SAIL, Ranchi (Jharkhand)-834 002, India. Contact e-mail: sp@rdcis.bih.nic.in.

2. Experimental Procedures

The alloys were air-melted in clay-bonded graphite crucibles in an induction furnace and sand cast into 25 mm diameter × 250 mm long cylindrical ingots. Chemical analysis (Table 1) was done with the help of a vacuum qantometer and x-ray fluorescence analysis.

Heat treatments were carried out in an air-tight muffle furnace, the temperature of which was controlled within ±5 °C. Thermo-gravimetric studies were carried out on NETZSCH Simultaneous Thermal Analyzer model STA 409 (Selb, Germany) using Keoline as reference material. The powder sample of the alloy weighing nearly 45 mg was taken in an alumina crucible and heated at a rate of 10 °C/min in air. The experimental data thus obtained were analyzed and plotted by the NETZSCH Data Acquisition System.

3. Results and Discussion

The microstructures of the experimental alloys (in the as-cast and in the heat-treated conditions) observed through optical metallography and x-ray diffractometry are summarized in the Tables 2 and 3.

Thermo-gravimetric (TG) data have been summarized in Tables 4 and 5 and in Fig. 1-3. From the tables and figures, the following inferences were drawn:

- 1) %TG increased very slowly with an increase in temperature. This was followed by an exponential increase on raising the temperature further (Fig. 1).
- 2) In the as-cast state, the weight gain was nearly a constant up to approximately 600 °C. %TG corresponding to this condition was a minimum for B2 followed by B1, B4, and B3. A steep increase in the %TG was observed at temperatures >600 °C, it being most marked in B2 followed by B4, B3, and B1 (Fig. 1).
- 3) In the 950 °C, 10 h, air cooled (AC) heat-treated condition,

Table 1 Chemical Analysis of Alloys, wt. %

Alloy	C	S	P	Si	Mn	Cr	Cu
B1	3.05	0.07	0.183	2.24	6.1	4.8	1.46
B2	2.90	0.065	0.173	2.14	7.5	4.8	1.48
B3	2.90	0.068	0.280	1.80	6.2	4.7	2.84
B4	2.85	0.072	0.305	1.80	7.3	4.5	2.86

Table 2 Summary of the Matrix Microstructure As Influenced by the Heat Treatments Analyzed Through Optical Metallography

Heat Treatment Schedule	Alloys			
	B1	B2	B3	B4
As-cast	P/B + M	B/M + RA	B/M + RA?	B/M + RA
900 °C, 4 h	A + M?	A	A + M?	A
900 °C, 10 h	A + M?	A	A + M?	A
950 °C, 4 h	A + M?	A	A + M?	A
950 °C, 10 h	A + M?	A	A + M?	A
1000 °C, 4 h	A	A	A	A
1000 °C, 10 h	A	A	A	A
1050 °C, 4 h	A	A	A	A
1050 °C, 6 h	A	A	A	A
1050 °C, 10 h	A	A	A	A

P, Pearlite; B, Bainite; M, Martensite; A, Austenite; RA, Retained Austenite

the weight gain was nearly a constant up to approximately 700 °C. %TG corresponding to this condition was a minimum for B2 followed by B3, B4, and B1 (Fig. 2).

- 4) In the 1050 °C, 10 h, AC heat-treated condition, the weight gain was nearly a constant up to approximately 800 °C. %TG corresponding to this condition was a minimum for B2 followed by B3, B1, and B4 (Fig. 3).

From a perusal of the thermo-gravimetric data (Fig. 1), it emerges that the TG data for as-cast microstructure has two distinct regions: (1) up to 600 °C and (2) beyond 600 °C and extending up to 1050 °C. The first of these is characterized by a very small and more or less uniform increase in %TG suggesting the usefulness of as-cast structure up to 600 °C. An equally important aspect is that whereas in the first temperature region the behavior of the alloy B2 was superior to others, there is a reversal of this trend in the second region (marked at temperature >700 °C) such that the increase in %TG is maximum in B2 followed by B3, B4, and B1. Thus, attention will focus on explaining this trend reversal and the difference in the high temperature response of the alloys.

To understand this, the TG data was re-examined in the context of critical/ transformation temperatures (Table 6). From this it emerges that the sharp increase in %TG between 1000 and 1050 °C may be directly related with the susceptibility to carbide transformation (M_5C_2 formation) in general, which is marked in B2 and B4 compared with B1 and B3. This is clearly demonstrated when percentage increase in TG is considered between the temperature ranges 900-1000 °C—actual temperatures representing carbide transformation are in the range of 890-935 °C (Table 6).

Table 3 Summary of the Presence of Carbides and Their Stability Ranges Analyzed Through X-Ray Diffractometry

Carbides	Stability Range(s)
M_3C	present up to 900 °C, 4 h
$M_{23}C_6$	present up to 950 °C, 4 h and at best in traces up to 950 °C, 10 h
M_5C_2	present up to 1000 °C, 10 h/1050 °C, 4 h
M_7C_3	present from 1000 °C, 10 h to 1050 °C, 10 h

The data show the percentage increase in TG to be a maximum in B2 followed by B4, B3, and B1. Between B1 and B3, the latter is more prone to the formation of M_5C_2 . Thus B1 is superior to all of the other alloys because it is less prone to form M_5C_2 type of carbide. A similar reasoning may explain the further sharp increase in %TG in B2, in comparison with the other alloys on heating to 1000-1050 °C.

The TG data further reflect upon the usefulness of the austenite-based microstructures in influencing high temperature behavior. This is clearly brought out by the lower %TG values observed in the temperature range 700-800 °C (structure austenite based) compared with those observed in the temperature range 600-700 °C (structure α based).

When the TG data for microstructures corresponding to 950 °C, 10 h and 1050 °C, 10 h AC heat treatments are compared, it is easy to assess why the microstructure corresponding to the latter is more effective upon heating to 800 °C. Because both of these heat treatments stabilize austenite and exclude the carbide transformations occurring around 900 °C, the present data once again favorably reflect on the usefulness of austenite-based structures and support the contention that the primary reason for the pronounced increase in the %TG is the carbide transformations.

The enrichment of parent austenite brought about by high temperature treatments must have further favorably contributed to the improved high temperature behavior of these microstructures compared with the behavior of the as-cast microstructure. Of the two heat treatments, the one carried out at 1050 °C enriched austenite more, besides also increasing its volume fraction. Accordingly, the high temperature behavior of microstructures attained on heat treating at 1050 °C would be superior to those attained on heat treating at 950 °C, as observed in the current study.

Looking to the overall deductions based on the TG data, it is evident that where the microstructure is austenite-based, the high temperature behavior would be controlled by the stability of austenite and the proneness of the alloys to carbide transformations. Because these two factors are a function of the alloy content, the behavior of the experimental alloys is expected to differ from one another. Where the matrix is not austenitic, other factors need consideration (e.g., an alloy with a martensitic matrix or a partly martensitic matrix may respond favorably to high temperatures as long as martensite decomposition has not occurred). Thereafter, its behavior will depend on the decomposition kinetics of martensite. On the other hand, an alloy that is not fully martensitic to begin with may not respond as favorably to high temperatures as the alloy in the earlier instance, but its behavior is likely to be more consistent

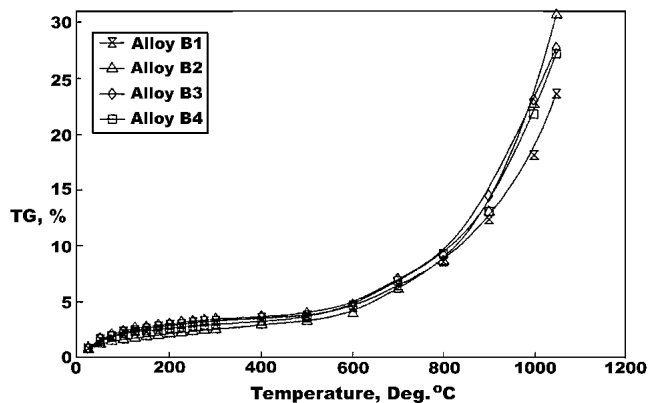


Fig. 1 Thermo-gravimetric data on experimental alloys in the as-cast state

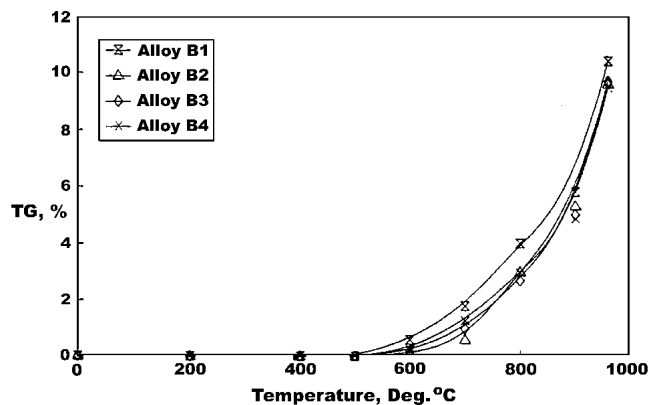


Fig. 2 Thermo-gravimetric data on experimental alloys in the 950 °C, 10 h, AC condition

Table 4 Effect of Heating Temperature on the %TG

Alloy	Heating Temperature, °C											
	RT	100	200	300	400	500	600	700	800	900	1000	1050
B1	0.0	2.5	3.1	3.27	3.27	3.88	4.49	6.48	8.62	12.37	18.11	23.62
B2	0.0	1.52	2.51	2.58	3.03	3.27	4.03	6.15	8.66	13.10	22.66	30.71
B3	0.0	2.31	3.07	3.38	3.53	4.00	4.78	7.07	9.22	14.47	23.07	27.69
B4	0.0	2.15	2.64	2.96	3.22	3.63	4.70	6.93	9.25	13.15	21.78	27.23

RT, room temperature

Table 5 Percentage Increase in %TG on Heating in the Different Temperature Ranges

Alloy	Temperature Range										
	I	II	III	IV	V	VI	VII	VIII	IX	X	XI
B1	...	24.0	5.5	0.0	18.6	15.7	44.3	33.0	43.5	46.4	30.4
B2	...	65.1	2.8	17.4	7.9	23.2	52.6	40.8	51.3	73.0	35.5
B3	...	32.9	10.1	4.4	13.3	19.5	47.9	30.4	56.9	59.4	20.0
B4	...	22.8	12.1	8.8	12.7	29.5	47.4	33.5	41.1	66.9	25.0

compared with a martensite-bearing alloy that would undergo softening after the martensite has decomposed. A somewhat similar reasoning may account for the overall superiority of B2 and B4 (more so of B2) over B1 and B3 up to about 500-600 °C and a marginally improved performance of B1 thereafter up to 700 °C. Reasons for differences in high temperature response beyond 700 °C have already been discussed. It would nonetheless be appropriate to state that the interpretation of the overall high temperature behavior may not be as simplistic. Furthermore, a clearer picture would have emerged if the P content of the four alloys were identical.

4. Modeling of the TG Data

The above discussion essentially dealt with the high temperature response of some selected microstructures and of the possible impact of various transformations, occurring during heating, in affecting the overall high temperature behavior.

Now, looking into the modeling aspect of the TG data, it would be necessary to examine the processes involving high temperature oxidation per se and arrive at the possible rate laws relevant to the current study, which would eventually form the basis of modeling.

Oxidation of metals can be expressed by a simple chemical reaction as:



However, the reaction path and the oxidation behavior of a metal may depend on a variety of factors, and reaction mechanism(s) may as a result prove complex. Initial oxide formation is a function of surface orientation and condition, concentration of crystal defects at the surface, and impurities in both the metal and the gas.

For a particular metal, the reaction mechanism is a function of the pre-treatment and surface condition, temperature, gas composition and pressure, and elapsed time of reaction. Looking to the possibility of a large variation in the properties of

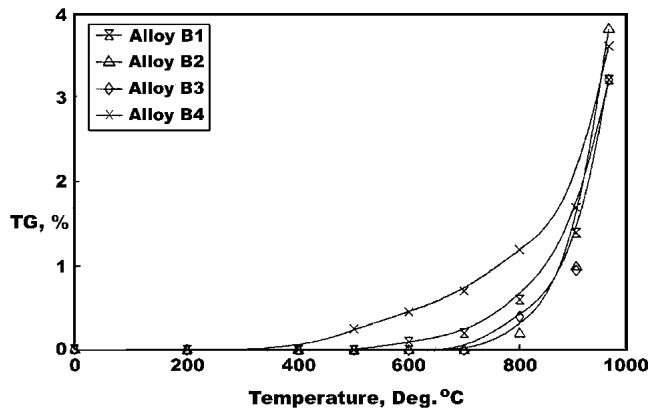


Fig. 3 Thermo-gravimetric data on experimental alloys in the 1050 °C, 10 h, AC condition

different metals and alloys and their oxides, a number of theories are needed to describe the oxidation behavior of metals.

A scrutiny of Fig. 1 revealed that although the %TG varies exponentially with temperature, the plot has two distinct parts, the nature of variation in one being opposite to that of the other. The first part (from ambient temperature to 200 °C) can be represented by an asymptotic curve as:

$$\%TG = A1' \cdot (\exp^{-T/A2'} - 1) \quad (\text{Eq 3})$$

and the second part follows an Arrhenius-type equation, which can be represented as:

$$\%TG = A1 + A2 \cdot \exp^{-A3/T} \quad (\text{Eq 4})$$

where, A1', A2', A1, A2, and A3 are constants, and T is temperature in K.

The %TG increase in the first part is very small (~2%) compared with the overall increase of up to (~27-30%) attained at highest heating temperature. It was, therefore, felt appropriate to neglect the former in arriving at the proposed model. The multi-variable nonlinear constraint optimization technique was used to calculate the constants. The correlations thus obtained are summarized as follows:

$$\text{Alloy B1} \quad \%TG = 1.561878 + 2665.150 \exp^{-7529.676/T} \quad (\text{Eq 5})$$

$$\text{Alloy B2} \quad \%TG = 1.310813 + 9623.292 \exp^{-8771.445/T} \quad (\text{Eq 6})$$

$$\text{Alloy B3} \quad \%TG = 1.515658 + 3465.314 \exp^{-7609.409/T} \quad (\text{Eq 7})$$

$$\text{Alloy B4} \quad \%TG = 1.566102 + 4004.606 \exp^{-7792.101/T} \quad (\text{Eq 8})$$

The %TG calculated from the aforesaid correlation revealed that predicted data are within +6% of the experimentally determined data for the alloys B1 and B3 and within +10% for the

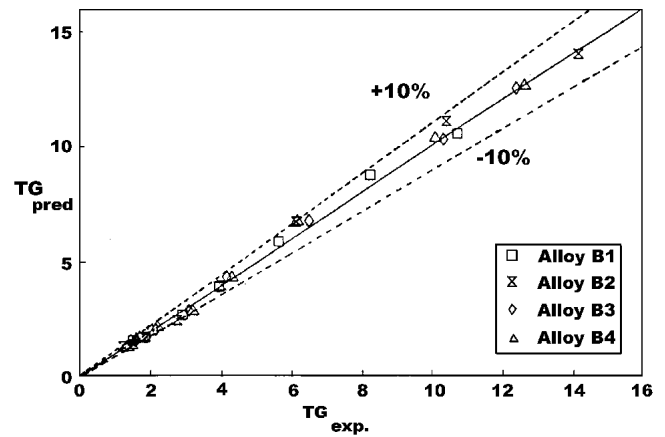


Fig. 4 A plot of experimental versus predicted %TG based on the models developed

Table 6 Critical/Transformation Temperatures

Alloys	Temperature, °C		
	I	II	III
B1	722	935	...
B2	750	920	1050
B3	745	890	...
B4	735	925	1075

alloys B2 and B4 (Fig. 4). This scatter is within a small range and therefore favorably reflects upon the validity of the model.

An examination of the above model revealed that the constant A1, which represents the base of the plot, varies within a close range (i.e., ~1.31~1.57), it being a minimum for alloy B2. This clearly indicates why alloy B2 has proved best initially. The constant A2, which represents the slope of the plot (i.e., the rate of increase in %TG), varies from ~2665 to ~9623, it being maximum for B2. This also agrees with the experimental findings that the rate of increase in %TG was maximum for the alloy B2, and this tendency was marked at higher temperatures. The third constant, which represents the exponential nature of the plot, varies over a close range (i.e., between ~8771 to ~7529) thereby suggesting that the nature of the %TG increase for all the alloys should be similar. The experimental data are in consonance with this analysis. The model is thus physically consistent.

5. Summary

These data reflect on the superiority of austenite-based microstructures in withstanding high temperatures (>700 °C). The higher the volume fraction of austenite and the larger its stability, the better would be the high temperature response. The morphology and stability of the second phase are equally important. The larger the proneness of the alloys to carbide transformation, the higher its adverse effect on the high temperature response. Martensite-based structures are useful up to ~500 °C. Between this stage and 700 °C, a non-martensitic structure will

prove more useful; it does not undergo as marked a softening as is observed on the decomposition of martensite. The present alloys are merely the first among the set of alloys being developed. Substantially improved high temperature performance can be expected from Fe-Mn-Cr-Cu alloys because there is a considerable scope to enhance the alloy content and to simultaneously implement the guidelines summarized in the conclusions. These guidelines were not considered while designing the present alloys, as the primary basis of designing them was to attain the best resistance to corrosion relative to the amount of alloying elements used.

6. Conclusions

Under the existing experimental conditions the following conclusions may be arrived at:

- 1) The as-cast microstructure is suitable up to 600 °C.
- 2) On heat treating from 950 °C (10 h holding followed by air cooling), the usefulness of the alloys was extended up to 700 °C.
- 3) On imparting the 1050 °C (10 h, AC) heat treatment, the usefulness of the alloys was extended to 800 °C.
- 4) The relative performance of the experimental alloys was a function of the stability and volume fraction of the austenite (i.e., matrix and the proneness of the alloys to carbide transformations occurring in the range of 890-935 °C and between 1050-1075 °C) (only in 82 and 84).
- 5) A mathematical model, developed to interrelate the weight gain with temperature, is of the form:

$$TG = A1.exp^{(-a2/T)}$$

The final models are:

$$\begin{aligned} \text{Alloy B1} \quad \%TG &= 1.561878 + 2665.150 \exp^{(-7529.676/T)} \\ \text{Alloy B2} \quad \%TG &= 1.310813 + 9623.292 \exp^{(-8771.445/T)} \\ \text{Alloy B3} \quad \%TG &= 1.515658 + 3465.314 \exp^{(-7609.409/T)} \\ \text{Alloy B4} \quad \%TG &= 1.566102 + 4004.606 \exp^{(-7792.101/T)} \end{aligned}$$

References

1. L.L. Shreir, ed.: "Cast Irons" in *Corrosion*, Vol. 1, Newnes and Butterworths, London, UK, 1977, pp. 3:85-3:97, 3:111-3:117.
2. R.S. Gundlach and D.V. Doane: "Alloy Cast Irons—Properties and Selection: Irons, Steels and High Performance Alloys" in *Metals Handbook*, Vol. 1, 10th ed., ASM International, Metals Park, OH, 1990, pp. 88-89.
3. Anon: "Ni-Resist Austenitic Cast Irons: Properties and Applications, International Nickel Co., Ltd., New York, NY, 1965, pp. 1-21.
4. R.S. Gundlach and D.V. Doane: "Alloy Cast Irons—Properties and Selection: Irons, Steels and High Performance Alloys" in *Metals Handbook*, Vol. 1, 10th ed., ASM International, Metals Park, OH, 1990, p. 103.
5. V. Kumar, P. Prasada Rao, and A.K. Patwardhan: "New Developments in Corrosion Resistant Alloys for Marine Applications," *Mater. Perform.*, 1991, 30, pp. 72-74.
6. V. Kumar, P. Prasada Rao, and A.K. Patwardhan: "Alloy White Iron—A New Approach to the Design and Development of Corrosion Resistant Materials for Marine Environments" in *Proc. of International Conference on Corrosion and Corrosion Control for Offshore and Marine Construction*, 1988, pp. 623-28.
7. V. Kumar and A.K. Patwardhan: "Effect of Microstructure on the Corrosion Behavior of 6% Cr White Iron Alloyed With Mn and Cu," *Corrosion*, 1993, 49, pp. 464-72.
8. V. Kumar and A.K. Patwardhan: "Electrochemical Characterization of a Corrosion-Resistant Cast White Iron," *Mater. Perform.*, 1993, 32, pp. 66-69.
9. V. Kumar and A.K. Patwardhan: "A New Method of Preparing Iso-Hardness Plots," *J. Mater. Eng. Perform.*, 1993, 2, pp. 51-55.